Characterization and Antibacterial Activity of Silver-Manganese Bimetallic Nanoparticles Biofabricated Using *Arachis Pintoi* Extract

Huynh Van Tien[1], Nguyen Tri[2,3]*, Nguyen Phung Anh[3], Dang Mai Nhi[3], Le Thi Bich Hang[2], Duong Nhat Linh[2], Nguyen Van Minh[2]

[1] Ho Chi Minh City University of Food Industry, Ho Chi Minh City, Vietnam
[2] Ho Chi Minh City Open University, Ho Chi Minh City, Vietnam
[3] Institute of Chemical Technology-VAST, Ho Chi Minh City, Vietnam.

ABSTRACT

This is the first time the bimetallic Ag-Mn nanoparticles – (Ag-Mn)NPs were synthesized using *Arachis pintoia* extract. The obtained samples were characterized and analyzed by various techniques, including X-Ray Diffraction, TEM, and FT-IR. XRD analysis confirmed the crystalline nature of nanoparticles. TEM images showed that the samples were nearly spherical in shape and uniform in size distribution with the average nanosizes of 3.3 nm for bimetallic (Ag-Mn)NPs, and 11.8 nm for monometallic AgNPs. FT-IR confirmed that flavonoids, phenolic acids, and alkaloid molecules can be bound to NPs acted both as the reducing and stabilizing agents. The results suggested that (Ag-Mn)NPs showed much greater potential against bacteria than that of AgNPs.

Key Words: Antibacterial, Ag-Mn, bimetallic, nanoparticles, *Arachis pintoi.*

eIJPPR 2020; 10(1):70-76

HOW TO CITE THIS ARTICLE: Huynh Van Tien, Nguyen Tri, Nguyen Phung Anh, Dang Mai Nhi, Le Thi Bich Hang, Duong Nhat Linh, Nguyen Van Minh (2020). "Characterization and Antibacterial Activity of Silver-Manganese Bimetallic Nanoparticles Biofabricated Using *Arachis Pintoi* Extract", International Journal of Pharmaceutical and Phytopharmacological Research, 10(1), pp.70-76.

INTRODUCTION

The research in nanotechnology pledges quantum leaps not only in materials manufacturing and electronics but also possesses a lot of applications in healthcare, medicine, energy, and biotechnology. The use of the plant, algae, fungi, and bacteria provides eco-friendly, safe, reliable, and economical routes to synthesize nanoparticles (NPs). However, plant-mediated synthesis of nanoparticles is more advantageous compared to the methods that use microorganisms because they can be easily improved, are less biohazardous and are not involved in the elaborate stage of growing cell cultures [1]. Plants' parts like seeds [2], leaf [3], bark [4], stem [5] and fruit extracts [6] have been effectively used for synthesizing nanoparticles.

Metallic nanoparticles were classified as monometallic, bimetallic, and trimetallic nanopaticles. For preparation of bimetallic nanoparticles from precursor salts, two methods are adopted including co-reduction, and successive reduction [7]. Though a number of bimetallic nanoparticles have been synthesized through these processes, silver-manganese nanoparticles – (Ag-Mn)NPs are much less investigated although both are considered as antibacterial agents at the independent level. Manganese nanoparticles (MnNPs) have proven to be effective against bacteria. In the context of monometallic MnNPs, their easy fabrication, environment affable nature and the non-toxic means of synthesis make MnNPs one of the best alternatives for a number of biological uses. They possess antibacterial activity against broad spectrum microbes [8]. Green synthesis of MnNPs was reported in various publications. Employing plant extract as a reduction and stabilization agent of manganese metal into MnNPs is one of the simple, environment-friendly, and inexpensive approaches in green chemistry [8, 9]. Jayandran et al. [8] synthesized MnNPs by reducing manganese acetate using the lemon methanolic extract. The average crystallite size of nanoparticles was in the range of 50 nm. The antibacterial activities of MnNPs against Staphylococcus aureus, *Bacillus subtilis*, *Escherichia coli*, and

Corresponding author: Nguyen Tri
Address: Ho Chi Minh City Open University / Institute of Chemical Technology-VAST, Ho Chi Minh City, Vietnam
E-mail: ✉ ntri @ ict.vast.vn
Relevant conflicts of interest/financial disclosures: The authors declare that the research was conducted in the absence of any commercial or financial relationships that could be construed as a potential conflict of interest.
Received: 14 August 2019; **Revised:**06 January 2019; **Accepted:** 15 January 2020

Staphylococcus bacillus were appraised. The results showed that the antibacterial activities were superior for all bacteria. On the other hand, the antifungal activities of Mn NPs were studied against four fungal strains including Trichophyton simii, Curvularia lunata, Aspergillus niger, and Candida albicans. The results showed high antifungal activity against all fungal strains. Meanwhile, silver nanoparticles (AgNPs) exhibit the most efficient antibacterial and antifungal properties [10-12]. Antibacterial activity along with the mechanism of action of silver nanoparticles on both gram negative and gram positive bacteria, including Escherichia coli, Staphylococcus aureus, Bacillus subtilis, Streptococcus mutans, etc. has already been investigated [13]. The applications of both Mn and Ag nanoparticles validate the importance of both types of nanoparticles and require further exploration for the well-being of humans. However, no paper was published in the synthesis of (Ag-Mn)NPs through the green chemistry approach.

Arachis pintoi (A. pintoi) – a tropical legume has been originated from South America and has been widespread in the subtropics and wet tropics. It has been introduced to many areas including Argentina, Australia, Colombia and the USA, and countries in South-East Asia, Central America, and the Pacific. *A. pintoi* can be used as a ground cover as well as an ornament. *A. pintoi* is compatible with aggressive grasses such as Brachiaria and is tolerant of heavy grazing. Previous chemical analyses of the plant indicate the presence of phytosterols and flavonoids, phenolic acids, triterpenes, alkaloids, fatty acids, etc. [14]. These components can be used as a reducing agent in the preparation of nanoparticles. However, much less study of nanoparticle synthesis has been reported to date using *A. pintoi* extract as a combined reducing and stabilizing agent.

In this paper, Ag-Mn nanoparticles were synthesized by co-reduction of $AgNO_3$ and $KMnO_4$ solution using *A.pintoi* extract as a combined reducing and stabilizing agent. The physico-chemical properties of the obtained Ag-MnNPs were investigated. The antibacterial feature of silver nanoparticles was evaluated throughout against gam (–) bacteria including *Escherichia coli* (*E. coli*), *Salmonella typhimurium* (*Salmonella*), and *Pseudomanas aeruginosa* (*P. aeruginosa*); and gam (+) bacteria: *Staphylococcus aureus* (*S. aureus*) and *Bacillus cereus* (*B. cereus*).

MATERIAL AND METHODS

Preparation and Characterization of Sample

A. pintoi (both leaves and stems) were collected and washed several times with distilled water to eliminate the dust particles, and then ground to the fine powder in distilled water with the mass ratio of *A. pintoi*/water being 1/10. The mixture was boiled at 70 ºC for 2 hours to extract the reducing agents in the presence of leaves and stems of *A. pintoi*. The obtained extract was cooled to room temperature and then filtered with Whatman filter paper 0.22 µm before centrifuging at 5,000 rpm for 30 minutes to get rid of the heavy biomaterials. The extract was stored in the refrigerator at 4 ºC in order to be used for further experiments.

The AgNPs synthesis was performed by mixing silver nitrate ($AgNO_3$, Merck, >99.8%) solution with *A. pintoi* extract under stirring at room temperature and illuminated by the sunlight. According to our unpublished work, the suitable conditions for the synthesis of AgNPs using *A.pintoi* extract as reducing and stabilizing agent were determined such as $AgNO_3$ concentration of 1.75 mM, the volume ratio of $AgNO_3$ solution/A. pintoi extract of 4.0/1.0, stirring rate of 300 rpm and the synthesis duration of 90 minutes. The synthesis of Ag-Mn nanoparticles was performed similarly to the above with the ratios of $AgNO_3$ and $KMnO_4$ solutions followed by 2:1 and 1:1. The obtained Ag-Mn nanoparticles were symbolized (1Ag-1Mn)NPs and (1Ag-2Mn)NPs, respectively.

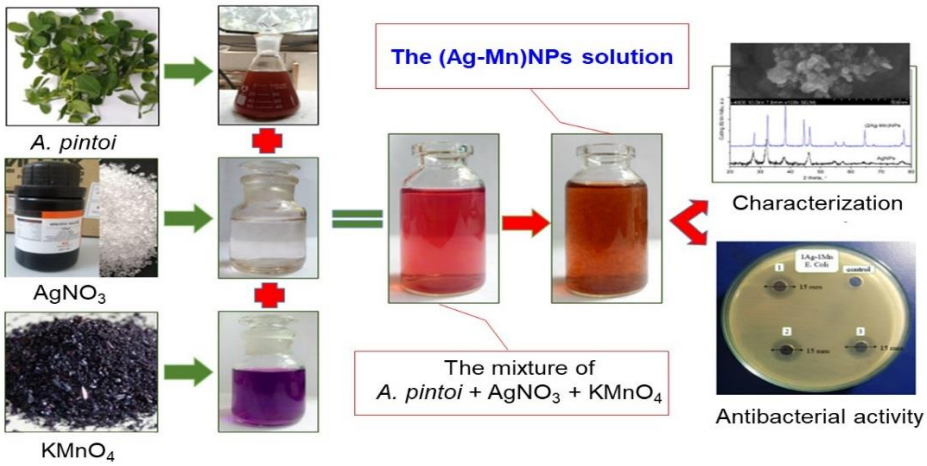

Figure 1. Illustration of the experimental process in biosynthesis of Ag-Mn bimetallic nanoparticles

The crystalline phases of the obtained AgNPs or (Ag-Mn)NPs powder which were washed and dried were determined by X–ray diffraction (XRD) using Bruker D2 Phaser powder diffractometer. The morphology of thesamples was characterized by transmission electron microscopy (TEM) using JEOL JEM 1400 instrument. A drop of the solution of samples was put on the carbon stub, dried and observed in TEM. The relation of nanoparticles with *A. pintoi* extract was investigated using Fourier transform infrared spectroscopy (FT-IR) carried out on a Tensor 27-Bruker spectrophotometer operating in the range of 400–4,000 cm^{-1} with resolution range of 2 cm^{-1}.

Antibacterial Activity

The obtained samples were tested for antibacterial activity against *E. coli*, *Salmonella*, *P. aeruginosa*, *S. aureus*, and *B. cereus* by the zone of inhibition and minimum inhibitory concentration which awere also stated in our previous work [15]. The bacterial strains were cultured with the Mueller-Hinton Agar (MHA) method, and then the strains were stored in the agar rods at 4 ºC. Three strains were added to the tube contained 5 mL pasteurized Trypticase Soy Broth (TSB) and statically cultured at 37 ºC in 18 hours. The paper discs were wetted by the solutions and allowed to dry, these dried discs then were placed on the agar. All the samples were stored in the refrigerator for 8 hours and finally incubated at 37 ºC for 18 hours. The antibacterial activity was recorded by measuring the diameter of the zone of inhibition around the agar.

RESULTS AND DISCUSSIONS

Characterization of the Synthesized Samples

The crystal structure of nanosamples was verified by XRD diffraction diagram (Fig.2). The results showed that the samples of AgNPs solution appeared at diffraction peaks at 38.1°; 46.1°, 64.1° and 76.9° corresponding to the plane (111), (200), (220) and (311) of the silver nanoparticles (JCPDS card No. 89-3722) [16]. In addition, a few intense and unassigned peaks at 2θ = 28.1°, 32.4°, 55.6°, and 57.0° in the vicinage of silver peaks exhibited the presence of bio-organic phase crystals [17], which were present in *A. pintoi* extract and responsible for silver ions reduction and stabilization of nanoparticles. Besides the appearance of AgNPs peak, the XRD diffractions of Ag-Mn samples also appeared at diffraction peaks at 38.4°, 46.4°, 57.6°, 64.6° and 77.8° characterized by the planes (310), (330), (510), (611), (721) of MnO_2 nanoparticles. On the other hand, the peaks at 2θ = 44.5° and 55.0° were characterized by the manganese crystal. Obviously, the crystallinity of the Ag-Mn samples is much higher than the AgNP sample.

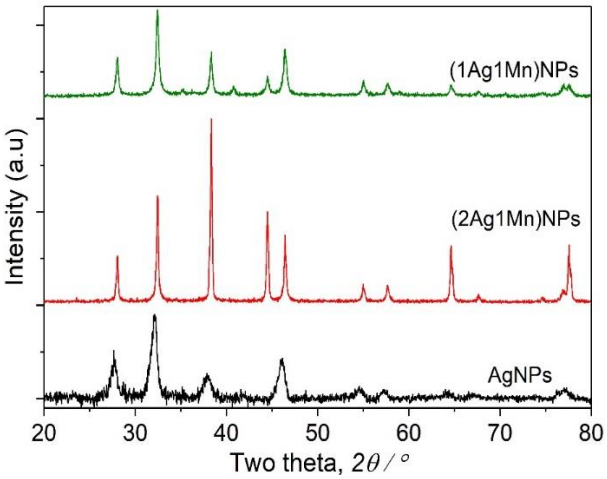

Figure 2. XRD patterns of the samples

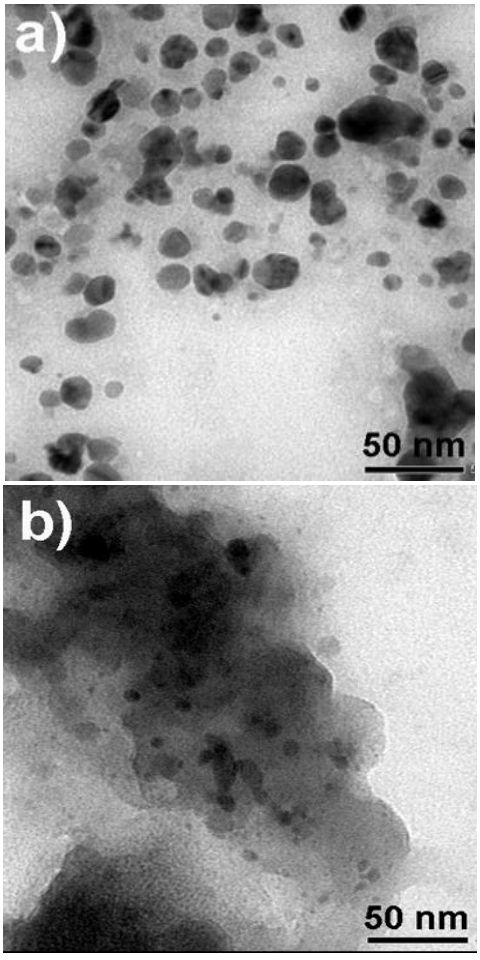

Figure 3. TEM images of AgNPs (a) and (2Ag-1Mn)NPs (b) samples

TEM image provided further insight into the morphology and size details of the formed nanoparticles. The result of the TEM image of the AgNPs sample (Fig.3a) indicated that nanoparticles were highly dispersed with a spherical shape size ranging of 0–40 nm. TEM images of the (2Ag-1Mn)NPs sample (Fig.3b) also showed similar results. The images clearly showed a bio-organic layer

coating around silver and manganese nanoparticles. This layer was due to surrounded phytochemicals in the extracts that served as a capping agent to prevent agglomeration. On the samples, silver and manganese nanoparticles mixed together had a relatively uniform size and were smaller than the pure AgNPs. Obviously, the sample (2Ag-1Mn)NPs has the smallest and most uniform particle size. From the TEM image, by using the ImageJ software, the size distribution of the samples was elucidated in Fig.4. The average sizes of AgNPs and (2Ag-1Mn)NPs were determined to be 11.8 and 3.3 nm, respectively.

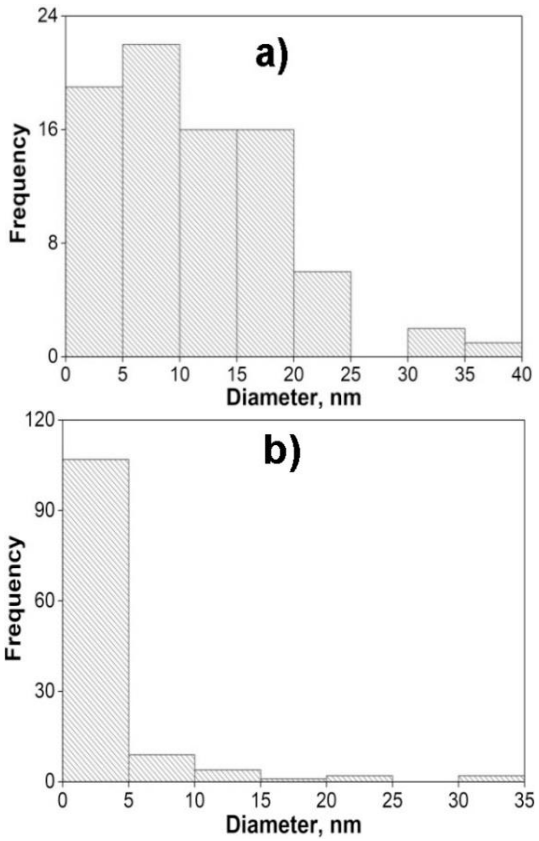

Figure 4. The size distribution histogram of AgNPs (a) and (2Ag-1Mn)NPs (b) samples

FT-IR spectra of *A. pintoi* extract, AgNPs solution, AgNPs powder, (1Ag-1Mn)NPs and (2Ag-1Mn)NPs powder were depicted in Fig.5. The spectrum for *A.pintoi* extract showed typical broad O-H stretching (3600–3300 cm^{-1}) and C=O stretching (1730–1690 cm^{-1}), suggesting the presence of flavonoids, phenolic acids, and alkaloids in extract that acted both as the reducing and stabilizing agents [18]. The difference was not much on the samples of pure *A. pintoi* extract and AgNPs solution. This could be because the compounds of *A. pintoi* extract covered the peaks of the silver nanoparticles by the functional groups contained in the extract, so the formation of the peaks of the silver nanoparticles was unclear. However, compared to pure *A. pintoi* extract, the FT-IR spectrum of AgNPs solution showed the presence of a weaker signals, proving the components of the extract reacted to form silver nanoparticles, so the concentration of the extract was significantly reduced. On the FT-IR spectrum of AgNPs and (2Ag-1Mn)NPs powder, a band centered at 2950 cm^{-1} was attributed to the axial stretching of C-H bonds, a peak at 1810 cm^{-1} was related to the axial stretching of C=O bonds of the acetamide groups, a peak at 1420 cm^{-1} corresponded to the symmetric angular deformation of CH_3, the band range of 1340–1440 cm^{-1} was assigned to CH_2 wagging and CH bending, the bands range of 1200–1300 cm^{-1} was associated with N–H bend amines and there was a broadband in the wavenumber range of 1153–897 cm^{-1} indicating the polysaccharide skeleton, including the vibrations of the glycoside bonds, C–O and C–O–C stretching. From the analysis of FT-IR studies, we confirmed that the flavonoids and alkaloids components together with phenolic acids in *A. pintoi* extract possibly performed dual functions for the formation and stabilization of AgNPs.

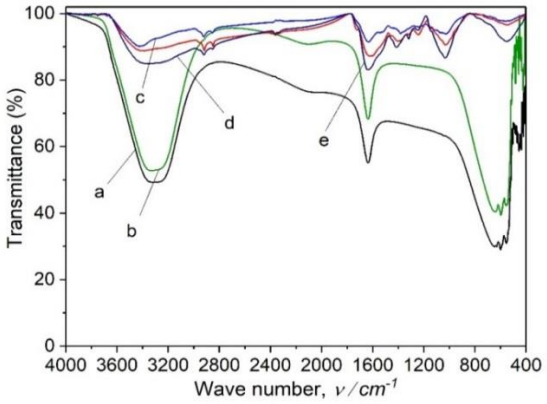

Figure 5. FT-IR spectra of *A. pintoi* extract (a), AgNPs solution (b), powder of AgNPs (c), (1Ag-1Mn)NPs (d), and (2Ag-1Mn)NPs (e)

Antibacterial Activity

The antibacterial activity of the samples was determined against *E. coli* bacterial strain on an agar plate. According to our unpublished work, the *A. pintoi* extract did not show any antibacterial activity against all tested bacteria. Fig.6 showed the inhibition zone of the samples against the bacteri. The samples showed good antibacterial activity against *E. coli*. Specifically, the average diameters of antibacterial rings were 12.3, 16.0, and 15.0 mm, respectively for AgNPs, (2Ag-1Mn)NPs, and (1Ag-1Mn)NPs. The bimetallic nanoparticles showed better antibacterial activity than the pure AgNPs. This may be due to the nature of Ag which is highly dispersed in the MnO_2 matrix, so that Ag can be more exposed to bacterial cells and shows potent antibacterial activity compared to bulk silver or AgNPs alone. Moreover, the advantage of incorporation of Ag into

MnO_2 lattice is the reduction of toxicity of free ions to human cells [19]. Obviously, the (2Ag-1Mn)NPs sample was the most outstanding. Appreciable antibacterial activity of (2Ag-1Mn)NPs is due to its nanosize and Mn^{4+}; whereas, the slightly lower antibacterial activity of (1Ag-1Mn)NPs is accredited to its higher nanosize and lower Mn^{4+} oxidation state in the sample as revealed by TEM and XRD analysis. Therefore, (2Ag-1Mn)NPs sample was chosen to investigate the inhibition zone against some other common bacterial strains.

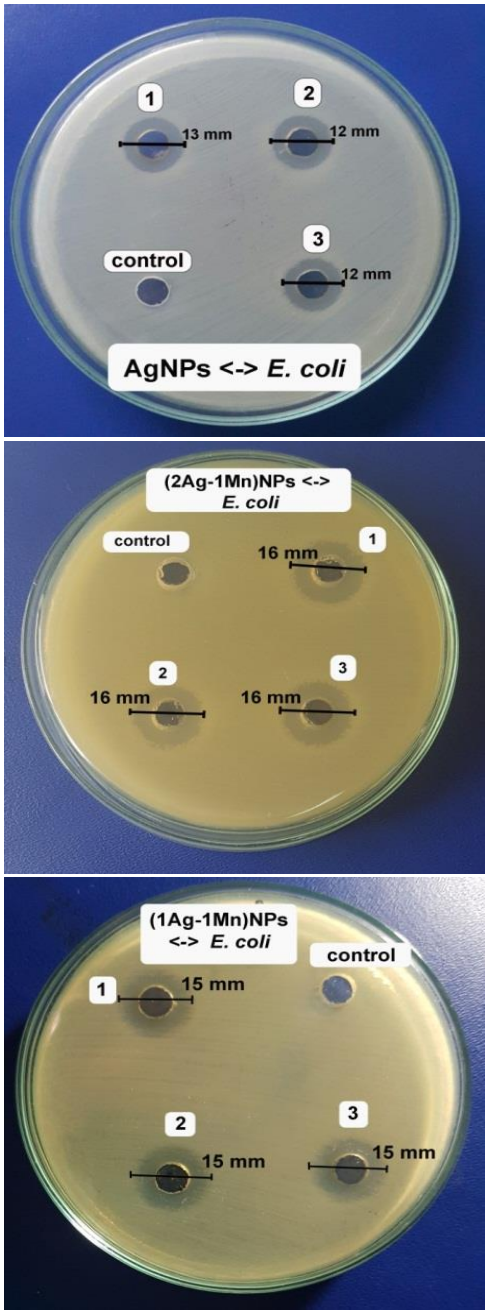

Figure 6. Images of inhibition zone of the samples against *E. coli*

The antibacterial activity of AgNPs and (2Ag-1Mn)NPs samples against *E.coli* was clearly shown in Fig.7. Indeed, not only the (2Ag-1Mn)NPs sample had a higher inhibition zone as mentioned above, but also the minimum inhibitory concentration (MIC) against *E. coli* was much lower than that of AgNPs (4.73 µg.mL^{-1} compared to 9.45 µg.mL^{-1}).

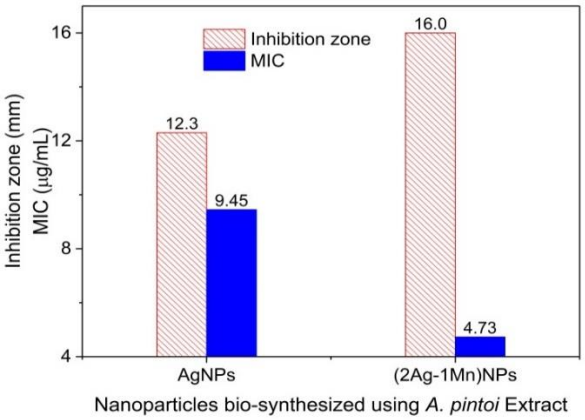

Figure 7. Images of inhibition zone and minimum inhibitory concentration (MIC) of AgNPs and (2Ag-1Mn)NPs samples against *E. coli*

The antibacterial activities of the (2Ag-1Mn)NPs sample were further determined against other bacteria strain (shown in Fig.8). The results showed high antibacterial activity against both gram (–) and gram (+) bacteria. The potent antibacterial properties of (2Ag-1Mn)NPs may be attributed to the released metal ions, which could have interaction with microorganisms by means of their attaching to the surface of the cell membranes of bacteria and penetrating into the bacterial cells. The zone of clearance observed against *Salmonella*, *P. aeruginosa*, *S. aureus*, and *B. cereus* was determined to be 17.7, 19.7, 14.0 and 16.0 mm, respectively.

The MIC values of (2Ag-1Mn)NPs against *Salmonella*, *P. aeruginosa*, *S. aureus*, and *B. cereus* are determined to be 4.73 µg.mL^{-1} similar to *E. coli*. Meanwhile, those for *Salmonella* and *P. aeruginosa* are only 2.37 µg.mL^{-1}. The above results show that gram (+) bacteria are less susceptible to Ag^+ than gram (–) bacteria. According to Dibrov [20], the NPs are positively charged, so they are convenient to attach to the negatively charged bacteria by electrostatic attraction in the cell membrane. In addition, the gram (+) bacterial cell wall was more peptidoglycan than that of gram (–) bacteria. As peptidoglycan is negatively charged and silver ions are positively charged, as the cell wall of gram (+) is thicker; a large number of silver nanoparticles may get stuck by peptidoglycan in gram (+) bacteria than in gram (–) bacteria [21]. Meanwhile, in gram (–) bacteria, the cell wall has a thinner peptidoglycan layer so the nanoparticles have a better antibacterial effect [22]. Ibrahim's work [23] also showed similar results for gram (–) and gram (+) bacteria strains.

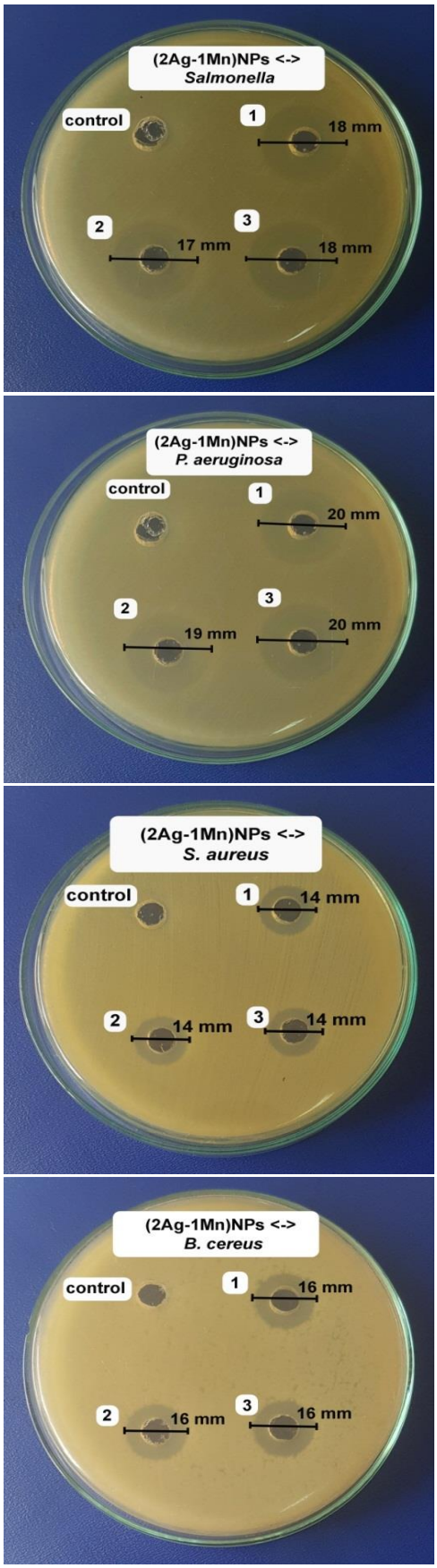

Figure 8. Images of inhibition zone of (2Ag-1Mn)NPs sample against *Salmonella*, *P. aeruginosa*, *S. aureus*, and *B. cereus*

CONCLUSIONS

The utilization of *A.pintoi* extract for the synthesis of monometallic and bimetallic nanoparticles under direct sunlight at room temperature proved to be efficient, rapid and environment-friendly. The characterized techniques of nanoparticles demonstrated the formation of highly crystalline particles possessing a spherical shape. The flavonoids, phenolic acids, and alkaloid groups from *A.pintoi* extract played a vital role in the reduction of Ag and Mn ions to bimetallic NPs, as well as the stabilization of the formed NPs. The results provide evidence that the bimetallic nanoparticles showed better antibacterial activity than the monometallic AgNPs, in which, the (2Ag-1Mn)NPs sample was the most outstanding. In this sample, the zone of clearance observed against *E. coli*, *Salmonella*, *P. aeruginosa*, *S. aureus*, and *B. cereus* was determined at the range of 14.0–19.7 mm. Hence, the properties of silver-manganese nanoparticles obtained from *A. pintoi* extract can unfasten new pathways in the development of new antibacterial agents derived from plant drugs.

REFERENCES

[1] Raut Rajesh W, Lakkakula Jaya R, Kolekar Niranjan S, Mendhulkar Vijay D, and Kashid Sahebrao B, 2009. Phytosynthesis of silver nanoparticle using Gliricidia sepium (Jacq.). Curr Nanosci. 5 (1), pp.117-122.

[2] Bar H, Bhui D K, Sahoo G P, Sarkar P, Pyne S, and Misra A, 2009. Green synthesis of silver nanoparticles using seed extract of Jatropha curcas. Colloids Surf. 348 (1), pp.212-216.

[3] Narayanan K B and Sakthivel N, 2008. Coriander leaf mediated biosynthesis of gold nanoparticles. Mater. Lett. 62 (30), pp.4588-4590.

[4] Sathishkumar M, Sneha K, Won S, Cho C-W, Kim S, and Yun Y-S, 2009. Cinnamon zeylanicum bark extract and powder mediated green synthesis of nano-crystalline silver particles and its bactericidal activity. Colloids Surf. B 73 (2), pp.332-338.

[5] Daisy P and Saipriya K, 2012. Biochemical analysis of Cassia fistula aqueous extract and phytochemically synthesized gold nanoparticles as hypoglycemic treatment for diabetes mellitus. Int. J. Nanomed. 7, pp.1189-1202.

[6] Ankamwar B, Damle C, Ahmad A, and Sastry M, 2005. Biosynthesis of gold and silver nanoparticles using Emblica officinalis fruit extract, their phase transfer and transmetallation in an organic solution. J. Nanosci. Nanotechnol. 5 (10), pp.1665-1671.

[7] Zaleska-Medynska A, Marchelek M, Diak M, and Grabowska E, 2016. Noble metal-based bimetallic

nanoparticles: the effect of the structure on the optical, catalytic and photocatalytic properties. Adv. Colloid Interface Sci. 229, pp.80-107.

[8] Jayandran M, Haneefa M M, and Balasubramanian V, 2015. Green synthesis and characterization of Manganese nanoparticles using natural plant extracts and its evaluation of antimicrobial activity. J. Appl. Pharm. Sci. 5 (12), pp.105-110.

[9] Quester K, Avalos-Borja M, and Castro-Longoria E, 2013. Biosynthesis and microscopic study of metallic nanoparticles. Micron 54, pp.1-27.

[10] Jaffri S B and Ahmad K S, 2018. Augmented photocatalytic, antibacterial and antifungal activity of prunosynthetic silver nanoparticles. Artif Cell Nanomed B 46 (sup1), pp.127-137.

[11] Al-thabaiti S A, Khan Z, and Manzoor N, 2015. Biosynthesis of silver nanoparticles and its antibacterial and antifungal activities towards Gram-positive, Gram-negative bacterial strains and different species of Candida fungus. Bioprocess Biosyst Eng 38 (9), pp.1773-1781.

[12] Phirange A S and Sabharwal S G, 2019. Green synthesis of silver nanoparticles using Fagopyrum esculentum starch: antifungal, antibacterial activity and its cytotoxicity. Indian J. Biotechnol. 18 (1), pp.52-63.

[13] Alsammarraie F K, Wang W, Zhou P, Mustapha A, and Lin M, 2018. Green synthesis of silver nanoparticles using turmeric extracts and investigation of their antibacterial activities. Colloids Surf. B 171, pp.398-405.

[14] Lopes R M, Agostini-Costa T d S, Gimenes M A, and Silveira D, 2011. Chemical composition and biological activities of Arachis species. J. Agric. Food Chem. 59 (9), pp.4321-4330.

[15] Linh D H, Anh N P, Mi T T, Tinh N T, Cuong H T, Quynh T L, Van N T, Minh N V, and Tri N, 2018. Biosynthesis, characteristics and antibacterial activity of silver nanoparticles using Lemon Citrus Latifolia extract. Mater Trans 59 (9), pp.1501-1505.

[16] Bykkam S, Ahmadipour M, Narisngam S, Kalagadda V R, and Chidurala S C, 2015. Extensive studies on X-ray diffraction of green synthesized silver nanoparticles. Adv. Nanopart. 4 (1), pp.1-10.

[17] AbdelHamid A A, Al-Ghobashy M A, Fawzy M, Mohamed M B, and Abdel-Mottaleb M M, 2013. Phytosynthesis of Au, Ag, and Au–Ag bimetallic nanoparticles using aqueous extract of sago pondweed (Potamogeton pectinatus L.). ACS Sustain Chem Eng 1 (12), pp.1520-1529.

[18] Bagherzade G, Tavakoli Maryam M, and Namaei Mohmmad H, 2017. Green synthesis of silver nanoparticles using aqueous extract of saffron (Crocus sativus L.) wastages and its antibacterial activity against six bacteria. Asian Pac J Trop Biomed 7 (3), pp.227-233.

[19] Kunkalekar R, Prabhu M, Naik M, and Salker A, 2014. Silver-doped manganese dioxide and trioxide nanoparticles inhibit both gram positive and gram negative pathogenic bacteria. Colloids Surf. B 113 pp.429-434.

[20] Dibrov P, Dzioba J, Gosink K K, and Häse C C, 2002. Chemiosmotic mechanism of antimicrobial activity of Ag+ in Vibrio cholerae. Antimicrob. Agents Chemother. 46 (8), pp.2668-2670.

[21] Lara H H, Ayala-Núnez N V, Turrent L C I, and Padilla C R, 2010. Bactericidal effect of silver nanoparticles against multidrug-resistant bacteria. World J. Microbiol. Biotechnol. 26 (4), pp.615-621.

[22] Shrivastava S, Bera T, Roy A, Singh G, Ramachandrarao P, and Dash D, 2007. Characterization of enhanced antibacterial effects of novel silver nanoparticles. Nanotechnology 18 (22), pp.103-112.

[23] Ibrahim H M, 2015. Green synthesis and characterization of silver nanoparticles using banana peel extract and their antimicrobial activity against representative microorganisms. J Radiat Res Appl Sc 8 (3), pp.265-275.